Modeling phototransformation reactions in surface water bodies: 2,4-Dichloro-6-nitrophenol as a case study

UNIVERSITÀ DEGLI STUDI DI TORINO

MODELLING PHOTOTRANSFORMATION REACTIONS IN SURFACE WATER BODIES: 2,4-DICHLORO-6-NITROPHENOL AS A CASE STUDY

Pratap Reddy Maddigapu,[1] Marco Minella,[1] Davide Vione,[1,2]* Valter Maurino,[1] Claudio Minero[1]

[1] *Dipartimento di Chimica Analitica, Università degli Studi di Torino, Via Pietro Giuria 5, 10125 Torino, Italy.*
[2] *Centro Interdipartimentale NatRisk, Università degli Studi di Torino, Via Leonardo da Vinci 44, 10095 Grugliasco (TO), Italy.*

* Corresponding author. E-mail: *davide.vione@unito.it*

Abstract

The anionic form of 2,4-dichloro-6-nitrophenol (DCNP), which prevails in surface waters over the undissociated one, has a direct photolysis quantum yield of $(4.53\pm0.78)\times10^{-6}$ under UVA irradiation and second-order reaction rate constants of $(2.8\pm0.3)\times10^{9}$ M^{-1} s^{-1} with $^{\bullet}OH$, $(3.7\pm1.4)\times10^{9}$ M^{-1} s^{-1} with $^{1}O_2$, and $(1.36\pm0.09)\times10^{8}$ M^{-1} s^{-1} with the excited triplet state of anthraquinone-2-sulphonate, adopted as a proxy for the photoactive dissolved organic compounds in surface waters. DCNP also shows negligible reactivity with the carbonate radical. Insertion of the data into a model of surface-water photochemistry indicates that the direct photolysis and the reactions with $^{\bullet}OH$ and $^{1}O_2$ would be the main phototransformation processes of DCNP, with $^{\bullet}OH$ prevailing in organic-poor and $^{1}O_2$ in organic-rich waters. The model results compare well with the field data of DCNP in the Rhône river delta (Southern France), where $^{1}O_2$ would be the main reactive species for the phototransformation of the substrate.

Introduction

The persistence in surface water bodies of dissolved organic compounds, including both natural organic molecules and man-made xenobiotics and pollutants, is influenced by their transformation kinetics due to abiotic and biotic processes, including light-induced reactions (*1*,*2*). The main photochemical pathways are direct photolysis, transformation sensitised by the triplet states of Coloured Dissolved Organic Matter (^{3}CDOM*), and reaction with photogenerated transients such as $^{\bullet}OH$, $CO_3^{-\bullet}$ and $^{1}O_2$ (*3*). The phototransformation kinetics depends on both substrate-related and ecosystem-related variables, namely photolysis quantum yield and reaction rate constants of the relevant compound, water

chemical composition and penetration of sunlight inside the water body, which is affected by absorbance and column depth (*4*,*5*).

Among the photogenerated transients, singlet oxygen is produced upon activation of ground-state oxygen by ^{3}CDOM* (*5*). The importance of $^1O_2$ in degradation reactions varies. For instance, $^1O_2$ would play a major role into the photodegradation of histidine and of 2- and 4-chlorophenolate (*6*,*7*). It is also important for the transformation of tryptophan, but probably less than ^{3}CDOM* (*6*,*7*). However, $^1O_2$ would not be able to significantly transform hardly oxidised compounds (*5*), including undissociated chlorophenols (*7*). The radical $CO_3^{-\bullet}$ is mainly generated by $^\bullet$OH and HCO_3^-/CO_3^{2-}. A usually less important pathway is the oxidation of carbonate by CDOM* (*8*). $CO_3^{-\bullet}$ would induce significant transformation of easily oxidised compounds (e.g. aromatic amines and sulphur-containing molecules) in carbonate-rich and DOM-poor waters (*9*). A relatively simple screening method to test the reactivity of an organic compound with $CO_3^{-\bullet}$ is the study of the effect of added bicarbonate in the presence of nitrate under irradiation (*10*,*11*).

The present study focuses on the phototransformation kinetics of 2,4-dichloro-6-nitrophenol (DCNP), an aromatic nitroderivative that has been detected in the Rhône river delta (Southern France) (*12*). DCNP is formed by photonitration of 2,4-dichlorophenol (DCP), which is an environmental transformation intermediate of the herbicide dichlorprop, used in flooded rice farming. DCNP can induce gene mutations and chromosomal aberrations (*13*,*14*) and acts as inhibitor of phenol sulfotransferase (*15*), which belongs to a class of enzymes that are involved in the detoxification of xenobiotics (*16*). The genotoxicity of DCNP is a typical feature of the aromatic nitroderivatives (*17*).

In this work, the photochemical reaction kinetics of DCNP was studied initially, assessing its direct photolysis quantum yield and the reactivity with $^\bullet$OH, $^1O_2$, $CO_3^{-\bullet}$ and ^{3}CDOM*. Anthraquinone-2-sulphonate (AQ2S) was chosen as a proxy for CDOM. A first reason for the choice is that quinone-like compounds are major components of the photoactive moieties of natural DOM, accounting for around 50% of the fluorescence of DOM samples (*18*). Moreover, the photochemistry and photophysics of AQ2S have been characterised in detail (*19*). The obtained kinetic parameters were then adopted as input data for a model that describes the photochemistry of the dissolved organic phase of surface waters. It was possible to predict the DCNP lifetime as a function of water chemical composition and column depth. Finally, the model results were compared with available field data of DCNP time evolution in the Rhône delta, the shallow waters of which are an environment where photochemical processes are supposed to play a key role in the transformation of dissolved organic pollutants (*12*).

Experimental

For reagents and materials see Supporting Information (hereafter SI). Solutions to be irradiated (5 mL) were placed inside Pyrex glass cells (4.0 cm diameter, 2.3 cm height, 295 nm cut-off) and magnetically

stirred during irradiation. The irradiation of DCNP + nitrate was carried out under a Philips TL 01 UVB lamp, with emission maximum at 313 nm (near the absorption maximum of nitrate) and 3.0±0.2 W m^{-2} UV irradiance in the 290-400 nm range, measured with a power meter by CO.FO.ME.GRA. (Milan, Italy). The incident photon flux in solution was 2.0×10^{-6} Einstein L^{-1} s^{-1}, actinometrically determined with the ferrioxalate method (*20*). The direct photolysis of DCNP and its sensitised phototransformation by AQ2S were studied under a set of five Philips TL K05 UVA lamps, with emission maximum at 365 nm, 60±1 W m^{-2} UV irradiance, and 5.7×10^{-5} Einstein L^{-1} s^{-1} incident photon flux in solution. The photodegradation of DCNP sensitised by Rose Bengal (RB) via $^1O_2$ was studied under a Philips TL K03 blue lamp, with emission maximum at 435 nm and 6.4×10^{-6} Einstein L^{-1} s^{-1} incident photon flux in solution. The lamp choice was based on exciting each photosensitiser as selectively as possible. The emission spectra of the lamps were taken with an Ocean Optics SD 2000 CCD spectrophotometer and normalised to the actinometry results, also taking into account the absorbance of the Pyrex glass walls of the irradiation cells. The absorption spectra of the relevant compounds were taken with a Varian Cary 100 Scan UV-Vis spectrophotometer. Figure 1A shows the overlap between the spectrum of the UVA lamp and that of DCNP at different pH values. Figure 1B shows the overlap between the UVA lamp spectrum and that of AQ2S, and between the blue lamp spectrum and that of RB. After irradiation, the solutions were analysed by High Performance Liquid Chromatography coupled with UV-Vis detection (HPLC-UV). For further details see SI.

Reaction rates were determined by fitting the time evolution data of DCNP with pseudo-first order equations of the form $C_t = C_o\ exp(-k\ t)$, where C_t is the concentration of DCNP at the time t, C_o its initial concentration, and k the pseudo-first order degradation rate constant. The initial degradation rate is $R_{DCNP} = k\ C_o$. Whenever relevant, the fit included the errors of the C_t vs. t data. The reported errors on the rates (±σ) represent the scattering of the experimental data around the fitting curve. The same applies to the error bounds associated to the values of the rate constants, where applicable. The reproducibility of repeated runs was around 10-15%. The data plots, the fits and the numerical integration to determine the absorbed photon fluxes were all carried out with the Fig.P software package.

Results and Discussion

Direct photolysis. DCNP 20 μM was irradiated under UVA at both pH 2.3 (undissociated DCNP) and pH 7.8 (phenolate). Note that DCNP has $pK_a \approx 4.75$ (*21*). Figure 1 shows that both forms of DCNP have $\varepsilon = (1.5\text{-}2.5)\times10^3$ M^{-1} cm^{-1} at 365 nm, which is the maximum emission wavelength of the lamp. Under such conditions, with an optical path length b = 0.4 cm, one gets an absorbance A = 0.012-0.020. Therefore, DCNP would absorb some (2.7-4.5)% of the incident radiation, a fraction that is lower than the errors on the determination of the degradation rate.

Figure 2 shows the time trend of DCNP as the average of triplicate runs. The initial transformation rate is R_{DCNP} = (4.62±0.78)×10^{-11} M s^{-1} at pH 2.3 and (1.05±0.18)×10^{-11} M s^{-1} at pH 7.8. Note that the error bars to the data in Figure 2 are relatively large, and the two data sets can be considered different only at p = 0.32 (t test). The fit of the two data series yielded different exponential functions, as shown by the 95% confidence bounds of the fit functions in Figure 2.

Figure 1 shows that the spectra of the lamp and of both forms of DCNP overlap in the 300-500 nm wavelength interval. It is possible to calculate the polychromatic quantum yield for the photolysis of DCNP by dividing R_{DCNP} for the absorbed photon flux (P_a^{DCNP}). The latter can be derived as follows (*22*):

$$P_a^{DCNP} = \int_{\lambda} p_a(\lambda)\, d\lambda = \int_{\lambda} p°(\lambda) \cdot \left[1 - 10^{-\varepsilon_{DCNP}(\lambda) \cdot b \cdot [DCNP]}\right] d\lambda \qquad (1)$$

where p°(λ) is the spectral photon flux density in solution (lamp spectrum, see Figure 1), $\varepsilon_{DCNP}(\lambda)$ the molar absorption coefficient of DCNP, and b = 0.4 cm the optical path length of the irradiated solution. One gets P_a^{DCNP} = 1.68×10^{-6} Einstein L^{-1} s^{-1} at pH 2.3 and 2.32×10^{-6} Einstein L^{-1} s^{-1} at pH 7.8. The polycromatic quantum yield is $\Phi_{DCNP} = R_{DCNP}\ (P_a^{DCNP})^{-1}$ = (2.75±0.46)×10^{-5} at pH 2.3 and (4.53±0.78)×10^{-6} at pH 7.8. The latter value is environmentally more significant because it is referred to the phenolate, which prevails in surface waters.

By comparison, the UV-Vis photolysis quantum yields of 2,4-dichlorophenol are 0.025 (undissociated phenol) and 0.26 (phenolate) (*23*). The corresponding values for 2,6-dichlorophenol are 0.034 and 0.22 (*23*). Note the faster direct photolysis of the dichlorophenolates. In the case of the undissociated 2- and 4-nitrophenol, the quantum yields were 8.4×10^{-5} and 3.3×10^{-4}, respectively (*24*). Finally, the quantum yield of 2,4-dinitrophenol was (8.1±0.4)×10^{-5} (undissociated compound) and (3.4±0.2)×10^{-5} (phenolate) (*25*).

Interestingly, the behaviour of DCNP toward direct photolysis resembles that of the nitrophenols rather than that of the chlorophenols. Moreover, the phenolate has lower photolysis quantum yield than the undissociated DCNP. The phenolates could undergo easier photoionisation than the corresponding phenols, which might partially explain the high photolysis quantum yield of the 2,4-dichlorophenolate (*2*). However, the direct phototransformation of the nitrophenols would rather take place via the reactions of the excited triplet states (*2,24*). Therefore, the lower Φ_{DCNP} of the phenolate may be caused by a less efficient formation or a lower reactivity of its triplet state compared to that of the undissociated phenol.

Reaction with $^{\bullet}$OH. The second-order rate constant between DCNP and $^{\bullet}$OH was assessed by competition with 2-propanol, using the UVB photolysis of nitrate as $^{\bullet}$OH source (*26*). Such a method

has already been adopted in the case of the nitrophenols (*24*). UVB irradiation of 20 µM DCNP + 10 mM NO_3^- was carried out with 2-propanol at concentration up to 1 mM, at pH 8.5 where the phenolate prevails. Figure 3 shows that the addition of 2-propanol inhibited the degradation of DCNP. Moreover, DCNP underwent negligible direct photolysis under the adopted conditions (UVB, pH 8.5, irradiation time up to 4 h). Photogenerated $^{\bullet}OH$ can react with either 2-propanol ($CH_3CHOHCH_3$), with second-order rate constant $k_3 = 1.9\times10^9$ M^{-1} s^{-1} (*27*), or DCNP:

$$NO_3^- + h\nu + H^+ \rightarrow {}^{\bullet}OH + {}^{\bullet}NO_2 \quad (2)$$

$$^{\bullet}OH + CH_3CHOHCH_3 \rightarrow H_2O + CH_3C^{\bullet}OHCH_3 \quad (3)$$

$$^{\bullet}OH + DCNP \rightarrow \text{products} \quad (4)$$

The competition kinetics foresees that the transformation rate of DCNP (R_{DCNP}) should decrease with increasing concentration of 2-propanol. However, in many cases there is some reaction between the substrate and the radicals that are formed by oxidation of the alcohol (*25*), which would yield a constant R_{DCNP} at elevated propanol. Let $R_{\bullet OH}$ be the formation rate of $^{\bullet}OH$ upon nitrate photolysis, c the constant rate term at elevated alcohol concentration, and k_4 the reaction rate constant between DCNP (phenolate) and $^{\bullet}OH$. Upon application of the steady-state approximation to $^{\bullet}OH$, one gets the following equation:

$$R_{DCNP} = \frac{R_{\bullet OH}\, k_4\, [DCNP]}{k_4\, [DCNP] + k_3\, [2-propanol]} + c \quad (5)$$

The fit of the experimental data with equation 5 yielded k_4 = (2.8±0.3)×10^9 M^{-1} s^{-1} and $R_{\bullet OH}$ = 8.0×10^{-10} M s^{-1} (see Figure 3). A similar experiment at pH 2 (undissociated DCNP) gave k_4 = 1.1×10^{10} M^{-1} s^{-1}. By comparison, the mononitrophenolates have $k_{\bullet OH}$ = 9.2×10^9 M^{-1} s^{-1} (2NP) and 3.8×10^9 M^{-1} s^{-1} (4NP) (*27*). In the case of 2,4-dinitrophenol, it was $k_{\bullet OH}$ = (1.76±0.05)×10^9 M^{-1} s^{-1} for the phenol and (2.33±0.11)×10^9 M^{-1} s^{-1} for the phenolate (*25*). Therefore, the reactivity of DCNP toward $^{\bullet}OH$ is comparable to that of the nitrophenols.

Reaction with $^1O_2$. Irradiation of Rose Bengal (RB) is a rather direct way to produce $^1O_2$ (*28*). The main $^1O_2$ sink is the energy loss upon collision with water (*5*), thus $^1O_2$ cannot be accumulated in solution and disappears if it does not react. Therefore, the reaction of any substrate with $^1O_2$ is in competition with the $^1O_2$ thermal deactivation. Note that significant quenching of $^1O_2$ photogenerated by DOM could take place at the DOM-water interface (*29*), which could influence the formation rate of $^1O_2$. In contrast, dissolved organic compounds are not able to compete with water for reaction with $^1O_2$ after it reaches the solution bulk, unless their concentration is very high (*5,30*). To calculate the

reaction rate constant between DCNP and $^1O_2$, RB should be irradiated in the presence of increasing [DCNP]. The following kinetic model is obtained:

$$RB + h\nu + O_2 \rightarrow {}^1O_2 \quad (6)$$

$$^1O_2 \rightarrow O_2 \quad (7)$$

$$DCNP + {}^1O_2 \rightarrow \text{products} \quad (8)$$

Let R_{1O2} be the formation rate of $^1O_2$ by RB, $k_7 = 2.5\times10^5$ s^{-1} the first-order thermal deactivation rate constant (*31*), k_8 the second-order reaction rate constant between DCNP and $^1O_2$, and R_{DCNP} the initial transformation rate of DCNP. Under the hypothesis that RB induces the transformation of DCNP only through photogenerated $^1O_2$, one gets:

$$R_{DCNP} = R_{^1O_2} \cdot \frac{k_8 \cdot [DCNP]}{k_8 \cdot [DCNP] + k_7} \quad (9)$$

The value of k_8 can be obtained from the curvature of R_{DCNP} vs. [DCNP] below a straight line at relatively elevated concentration of the substrate. However, DCNP is able to compete with RB for the lamp irradiance, and a screening effect of DCNP on RB would decrease R_{1O2} and produce a curvature as well. Therefore, it is important not to adopt too elevated [DCNP] values.

Figure 4 reports R_{DCNP} vs. [DCNP] upon blue-light irradiation of 20 µM RB at pH 8. The maximum adopted [DCNP] was 12.5 µM. In the presence of 12.5 µM DCNP, the photon flux absorbed by 20 µM RB would be decreased by less than 0.3% compared to RB alone, an effect that is below the experimental errors and can be neglected. Moreover, under the adopted experimental conditions the direct photolysis of DCNP was negligible. Figure 4 reports the fit of the experimental data with equation 9 (solid curve), which yields $k_8 = (3.7\pm1.4)\times10^9$ M^{-1} s^{-1}. See SI for the demonstration that DCNP actually reacts with $^1O_2$ in the presence of irradiated RB.

Reaction with $CO_3^{-\bullet}$. Figure 5 reports the initial degradation rate of 20 µM DCNP upon UVB irradiation of 10 mM $NaNO_3$, as a function of the concentration of added $NaHCO_3$. The Figure also reports the DCNP trend in the presence of a phosphate buffer (NaH_2PO_4 + Na_2HPO_4), at the same concentration as $NaHCO_3$ and same pH (±0.1 units), to differentiate the role of the bicarbonate/carbonate chemistry from the mere pH effect. Finally, the direct photolysis data are referred to systems containing DCNP + $NaHCO_3$, without nitrate. Bicarbonate slightly inhibits the degradation of DCNP, suggesting poor substrate reactivity toward $CO_3^{-\bullet}$. Overall, the effect of bicarbonate on DCNP is similar to that on 4-nitrophenol, which undergoes negligible reaction with $CO_3^{-\bullet}$ compared to $^\bullet$OH in surface waters (*11*).

Reaction with ^{3}CDOM*. The excited triplet states of CDOM are important reactive species in surface waters, also favoured by the major role of CDOM itself as radiation absorber. For instance, ^{3}CDOM* directs the transformation of electron-rich phenols (*32*) and phenylurea herbicides (*33*). The main difficulty is that CDOM is not a species of definite composition, thus it may be necessary to study the behaviour of molecules that are representative of the composition/reactivity of CDOM (*34*).

For this reason, we chose AQ2S as model molecule for CDOM, because ^{3}AQ2S* has the peculiarity not to react with O_2 and, therefore, not to yield $^1O_2$ (*19*,*35*).

Figure 6 reports the initial degradation rate of DCNP, UVA irradiated in the presence of 1 mM AQ2S at pH 8.5, as a function of [DCNP]. The direct photolysis of DCNP was negligible under the adopted irradiation time scale (up to 2 h). The experimental data of Figure 6 follow a straight line, suggesting that DCNP at the adopted concentration is a negligible scavenger of light-excited AQ2S. A further increase of [DCNP] is not recommended as it would induce an undesired competition for irradiance between AQ2S and DCNP. It is still possible to derive the reaction rate constant between ^{3}AQ2S* and DCNP, because the photochemistry of AQ2S is rather well known. First of all, the photon flux absorbed by 1 mM AQ2S is $P_a^{AQ2S} = \int_\lambda p_a^{AQ2S}(\lambda)\, d\lambda = 2.38 \cdot 10^{-5}\ Einstein\ L^{-1}\ s^{-1}$ (see eq.1 for comparison). From the data of Figure 6 the quantum yield of DCNP photodegradation by AQ2S is $\Phi_{DCNP}^{AQ2S} = R_{DCNP}^{AQ2S} \cdot (P_a^{AQ2S})^{-1} = (2.23 \pm 0.14) \cdot [DCNP]$. It is known from the literature that the quantum yield for the formation of ^{3}AQ2S* under UVA is $\Phi_{3AQ2S*} = 0.18$, and that the pseudo-first order decay constant of ^{3}AQ2S* is $k_{3AQ2S*} = 1.1 \times 10^7\ s^{-1}$ (*19*). Because ^{3}AQ2S* would either decay, or react with DCNP with rate constant $k_{DCNP}^{^3AQ2S*}$, the quantum yield of DCNP photodegradation would be $\Phi_{DCNP}^{AQ2S} = \Phi_{^3AQ2S*} \cdot k_{DCNP}^{^3AQ2S*} \cdot [DCNP] \cdot (k_{^3AQ2S*})^{-1}$, under the hypothesis that $k_{DCNP}^{^3AQ2S*} \cdot [DCNP] << k_{^3AQ2S*}$. By comparison with the expression of Φ_{DCNP}^{AQ2S} derived from Figure 6, one gets $\Phi_{^3AQ2S*} \cdot k_{DCNP}^{^3AQ2S*} \cdot (k_{^3AQ2S*})^{-1} = (2.23 \pm 0.14)$ and $k_{DCNP}^{^3AQ2S*} = (1.36 \pm 0.09) \cdot 10^8\ M^{-1}\ s^{-1}$. Note that this result is consistent with $k_{DCNP}^{^3AQ2S*} \cdot [DCNP] << k_{^3AQ2S*}$. An additional hypothesis is made here, that the reactivity of ^{3}AQ2S* + DCNP is representative of ^{3}CDOM* + DCNP.

Use of the kinetic data into the photochemistry model. The values of Φ_{DCNP} and of the rate constants with $^\bullet$OH, $^1O_2$ and ^{3}CDOM* were used as input data for a model, which describes photochemistry in the dissolved phase of surface waters as a function of chemical composition, absorption spectrum and column depth (*36*,*37*). For each photochemical pathway the model yields a half-life time τ_{DCNP}^{SSD} in summer sunny days (SSD), equivalent to a fair-weather 15 July at 45°N latitude, or a rate constant k_{DCNP}^{SSD} in SSD^{-1}, where $k_{DCNP}^{SSD} = \ln 2 \left(\tau_{DCNP}^{SSD}\right)^{-1}$. The details of the model for the relevant processes are described as SI, and only the results will be discussed here. As far as the direct photolysis is concerned, the rate constant of DCNP is:

$$(k_{DCNP}^{SSD})_{phot} = \frac{3.6 \cdot 10^7 \ \Phi_{DCNP} \int_{\lambda} p°(\lambda) \cdot [\,1 - 10^{-A_1(\lambda) \cdot d}\,] \cdot \frac{\varepsilon_{DCNP}(\lambda)}{A_1(\lambda)} \, d\lambda}{d} \qquad (10)$$

where d is the water column depth (in cm), Φ_{DCNP} = (4.53±0.78)×10^{-6}, $p°(\lambda)$ the spectrum of sunlight (in einstein cm^{-2} s^{-1} nm^{-1} and corresponding to 22 W m^{-2} UV irradiance, as can be observed in a sunny 15 July at 45°N latitude, at 10 am or 2 pm solar time, see Figure A-SI), $\varepsilon_{DCNP}(\lambda)$ the absorption spectrum of anionic DCNP (in M^{-1} cm^{-1}), and $A_1(\lambda)$ the specific absorbance (the absorbance value with b = 1 cm) of the surface water layer, where the sunlight irradiance is maximum and the photochemical processes are usually most favoured.

In the case of $^{\bullet}$OH, the rate constant of DCNP is:

$$k_{DCNP,{}^{\bullet}OH}^{SSD} = 3.6 \cdot 10^5 \, \frac{R_{{}^{\bullet}OH}^{tot} \, k_{DCNP,{}^{\bullet}OH}}{\sum_i k_{Si} \, [S_i]} \qquad (11)$$

where $\Sigma_i \, k_{Si} \, [S_i]$ is the rate constant of the natural $^{\bullet}$OH scavengers (in s^{-1}), $R_{{}^{\bullet}OH}^{tot}$ the formation rate of $^{\bullet}$OH inside a cylindrical volume of unit surface area and depth d (in M s^{-1}), and $k_{DCNP,{}^{\bullet}OH}$ = (4.2±0.4)×10^9 M^{-1} s^{-1}.

In the case of $^1O_2$, the rate constant of DCNP is:

$$k_{DCNP,{}^1O_2}^{SSD} = \frac{0.18 \cdot k_{DCNP,{}^1O_2} \cdot \int_{\lambda} p_a^{CDOM}(\lambda) \, d\lambda}{d} \qquad (12)$$

where $k_{DCNP,1O2}$ = (3.7±1.4)×10^9 M^{-1} s^{-1} and $p_a^{CDOM}(\lambda)$ is the spectral photon flux density absorbed by CDOM.

Finally, as far as ^{3}CDOM* is concerned, the rate constant is:

$$k_{DCNP,{}^3CDOM*}^{SSD} = \frac{0.092 \cdot k_{DCNP,{}^3CDOM*} \cdot \int_{\lambda} p_a^{CDOM}(\lambda) \, d\lambda}{d} \qquad (13)$$

where $k_{DCNP,3CDOM*}$ = (1.36±0.09)×10^8 M^{-1} s^{-1}.

Figure 7a reports the trend of k_{DCNP}^{SSD} as a function of the depth d and of the content of DOM (quantified as NPOC, non-purgeable organic carbon), in a water body that also contains 51 µM nitrate, 3.2 µM nitrite, 2.1 mM bicarbonate and 26 µM carbonate (in analogy with the lagoons of the Rhône river delta, Southern France (*12*)). Also note that the water spectrum $A_1(\lambda)$ was modelled from the

NPOC values (see SI for details). The rate constant is reported for the three most important processes (direct photolysis and reactions with $^{\bullet}OH$ and $^{1}O_2$), while the reaction with $^{3}CDOM^*$ was less significant. All the k_{DCNP}^{SSD} values decrease with increasing *d*, which is reasonable because the photochemical processes are most important in shallow waters. Moreover, direct photolysis and the reactions with $^{\bullet}OH$ and $^{1}O_2$ would all play a similar role for NPOC ≈ 2 mg C L^{-1}, $^{\bullet}OH$ would prevail at lower NPOC values, $^{1}O_2$ at higher NPOC. This finding suggests the importance of assessing all the main photochemical pathways involving a substrate in surface waters, because the prevailing transformation route could vary under different conditions.

Comparison between model results and field data. In the case of the Rhône delta water, DCNP is formed from DCP. The latter showed a concentration peak on 21 June 2005, while DCNP peaked in early July (*12*). The photochemical processes are very important in the transformation of dissolved pollutants in the Rhône delta (*12*,*38*), thus it is very interesting to compare the field data with the results of our model.

Figure 7b reports the time trend after 21 June of both DCP and DCNP in a ditch draining the paddy fields (*12*). The time choice has the purpose of simplifying the function describing DCP, to allow a workable solution of the DCNP differential equation (*vide infra*). The DCP trend follows a pseudo-first order kinetics, with $[DCP] = A\, exp(-k\, t)$, where *k* is the pseudo-first order transformation rate constant and *t* the time in days. The data fit yielded $A = 2.9 \cdot 10^{-8}$ M and $k = 0.12$ day^{-1}. On 21 June the concentration of DCNP is $C_o = 6.3 \cdot 10^{-9}$ M. DCNP is formed from DCP, and under a pseudo-first order approximation one can assume $d[DCNP]/dt = k'[DCP] - k''[DCNP]$. Here k" is the pseudo-first order transformation rate constant of DCNP, and $[DCP] = A\, exp(-k\, t)$. The solution of the resulting differential equation is:

$$[DCNP] = C_o\, e^{-k'' t} + \frac{k'\, A}{k'' - k} (e^{-k\, t} - e^{-k'' t}) \qquad (14)$$

The fit of the DCNP data in Figure 7b with equation 14 yielded k' = 0.098 day^{-1} and k" = 0.083 day^{-1}. The latter value can be compared with the model-derived DCNP transformation rate constant, k_{DCNP}.

The application of the photochemical model to the Rhône delta water, which contains 51 µM NO_3^-, 3.2 µM NO_2^-, 2.1 mM HCO_3^-, 26 µM CO_3^{2-} and 4.5 mg C L^{-1} NPOC (*12*), yields $k_{DCNP} = 0.11 \pm 0.04$ SSD^{-1} for the main transformation pathway (DCNP + $^{1}O_2$). The other pathways yielded significantly lower rate constants. From these data one can conclude that: *(i)* the main transformation pathway of DCNP in the Rhône delta is the reaction with $^{1}O_2$, and *(ii)* the model value of k_{DCNP} is compatible with the pseudo-first order transformation rate constant k", derived from the DCNP field monitoring. Note that 1 day ≈ 1 SSD in the relevant period (June-July).

Acknowledgements

Financial support by PNRA-Progetto Antartide and INCA consortium is gratefully acknowledged. The work of PRM in Torino was supported by a Marie Curie International Incoming Fellowship (IIF), under the FP7-PEOPLE programme (contract n° PIIF-GA-2008-219350, project PHOTONIT).

Literature Cited

1) Bucheli-Witschel, M.; Egli, T. Environmental fate and biodegradation of aminopolycarboxylic acids. (2001) *FEMS – Microb. Rev.* **2001**, *25*, 69-106.
2) Boule, P.; Bahnemann, D.; Robertson, P. J. K. (eds.), *Environmental Photochemistry Part II (The Handbook of Environmental Chemistry Vol. 2M)*, , Springer, Berlin, 2005.
3) Czaplicka, M. Photo-degradation of chlorophenols in the aqueous solution. *J. Haz. Mat.* **2006**, *134*, 45-59.
4) Loiselle, S.; Bracchini, L.; Dattilo, A. M.; Ricci, M.; Tognazzi, A.; Cozar, A.; Rossi, C. Optical characterization of chromophoric dissolved organic matter using wavelength distribution of absorption spectral slopes. *Limnol. Oceanogr.* **2009**, *54*, 590-597.
5) Hoigné, J. Formulation and calibration of environmental reaction kinetics: Oxidations by aueous photooxidants as an example. In *Aquatic Chemical Kinetics*; Stumm, W., Ed., Wiley: New York, 1990; pp 43-70.
6) Boreen, A. L.; Edhlund, B. L.; Cotner, J. B.; McNeill, K. Indirect photodegradation of dissolved free amino acids: The contribution of singlet oxygen and the differential reactivity of DOM from various sources. *Environ. Sci. Technol.* **2008**, *42*, 5492-5498.
7) Vione, D.; Bagnus, D.; Maurino, V.; Minero, C. Quantification of singlet oxygen and hydroxyl radicals upon UV irradiation of surface water. *Environ. Chem. Lett.* **2010**, *8*, 193-198.
8) Canonica, S.; Kohn, T.; Mac, M.; Real, F. J.; Wirz, J.; von Gunten, U. Photosensitizer method to determine rate constants for the reaction of carbonate radical with organic compounds. *Environ. Sci. Technol.* **2005**, *39*, 9182-9188.
9) Huang, J. P.; Mabury, S. A. Steady-state concentrations of carbonate radicals in field waters. *Environ. Toxicol. Chem.* **2000**, *19*, 2181-2188.
10) Bouillon, R. C.; Miller, W. L. Photodegradation of dimethyl sulfide (DMS) in natural waters: Laboratory assessment of the nitrate-photolysis-induced DMS oxidation. *Environ. Sci. Technol.* **2005**, *39*, 9471-9477.
11) Vione, D.; Khanra, S.; Cucu Man, S.; Maddigapu, P. R.; Das, R.; Arsene, C.; Olariu, R. I.; Maurino, V.; Minero, C. Inhibition vs. enhancement of the nitrate-induced phototransformation of

organic substrates by the $^{\bullet}$OH scavengers bicarbonate and carbonate. *Wat. Res.* **2009**, *43*, 4718-4728.

12) Chiron, S.; Minero, C.; Vione, D. Occurrence of 2,4-dichlorophenol and of 2,4-dichloro-6-nitrophenol in the Rhône river delta (Southern France). *Environ. Sci. Technol.* **2007**, *41*, 3127-3133.
13) Heng, Z.C.; Nath, J.; Liu, X.R.; Ong, T. Induction of chromosomal aberrations by 2,4-dichloro-6-aminophenol in cultured V79 cells. *Teratogen. Carcinogen. Mutagen.* **1996**, *16*, 81-87.
14) Heng, Z.C.; Ong, T.; Nath, J. In vitro studies of the genotoxicity of 2,4-dichloro-6-nitrophenol ammonium (DCNPA) and its major metabolite. *Mutat. Res.* **1996**, *368*, 149-155.
15) Kroegerkoepke, M.B.; Koepke, S.R.; Hernandez, L.; Michejda, C.J. Activation of a beta-hydroxyalkylnitrosamine to alkylating agents – Evidence for the involvement of a sulfotransferase. *Cancer Res.* **1992**, *52*, 3300-3305.
16) Wang, L.Q.; James, M.O. Inhibition of sulfotransferases by xenobiotics. *Curr. Drug Metab.* **2006,** *7*, 83-104.
17) Chiron, S.; Barbati, S.; De Méo, M.; Botta, A. In vitro synthesis of 1,N^6-etheno-2'-deoxyadenosine and 1,N^2-etheno-2'-deoxyguanosine by 2,4-dinitrophenol and 1,3-dinitropyrene in the presence of a bacterial nitroreductase. *Environ. Toxicol.* **2007**, *22*, 222-227.
18) Cory, R. M.; McKnight, D. M. Fluorescence spectroscopy reveals ubiquitous presence of oxidized and reduced quinones in dissolved organic matter. *Environ. Sci. Technol.* **2005**, *39*, 8142-8149.
19) Loeff, I.; Treinin, A.; Linschitz, H. Photochemistry of 9,10-anthraquinone-2-sulfonate in solution. 1. Intermediates and mechanism. *J. Phys. Chem.* **1983**, *87*, 2536-2544.
20) Kuhn, H. J.; Braslavsky, S. E.; Schmidt, R. Chemical actinometry. *Pure Appl. Chem.* **2004**, *76*, 2105-2146.
21) Aptula, A. O.; Netzeva, T. I.; Valkova, I. V.; Cronin, M. T. D.; Schultz, T. W.; Kühne, R.; Schüürmann, G. Multivariate discrimination between modes of toxic action of phenols. *Quant. Struct.-Activ. Relat.* **2002**, *21*, 12-22.
22) Braslavsky, S.E. Glossary of terms used in photochemistry, 3rd edition. *Pure Appl. Chem.* **2007**, *79*, 293-465.
23) Vione, D.; Minero, C.; Housari, F.; Chiron, S. Photoinduced transformation processes of 2,4-dichlorophenol and 2,6-dichlorophenol on nitrate irradiation. *Chemosphere* **2007**, *69*, 1548-1554.
24) Vione, D.; Maurino, V.; Minero, C.; Duncianu, M.; Olariu, R. I.; Arsene, C.; Sarakha, M.; Mailhot, G. Assessing the transformation kinetics of 2- and 4-nitrophenol in the atmospheric aqueous phase. Implications for the distribution of both nitroisomers in the atmosphere. *Atmos. Environ.* **2009**, *43*, 2321-2327.
25) Albinet, A.; Minero, C.; Vione, D. Phototransformation processes of 2,4-dinitrophenol, relevant to atmospheric waters. *Chemosphere* **2010**, *80*, 753-758.

26) Mack, J.; Bolton, J. R. Photochemistry of nitrite and nitrate in aqueous solution: A review. *J. Photochem. Photobiol. A-Chem.* **1999**, *128*, 1-13.
27) Buxton, G. V.; Greenstock, C. L.; Helman, W. P.; Ross, A. B. Critical review of rate constants for reactions of hydrated electrons, hydrogen atoms and hydroxyl radicals ($^{\bullet}OH/^{\bullet}O^{-}$) in aqueous solution. *J. Phys. Chem. Ref. Data* **1988**, *17*, 1027-1284.
28) Miller, J. S. Rose-bengal sensitized photooxidation of 2-chlorophenol in water using solar simulated light. *Wat. Res.* **2005**, *39*, 412-422.
29) Latch, D. E.; McNeill, K. Microheterogeneity of singlet oxygen distribution in irradiated humic acid solutions. *Science* **2006**, *311*, 1743-1747.
30) Cory, R. M.; Cotner, J. B.; McNeill, K. Quantifying interactions between singlet oxygen and aquatic fulvic acids. *Environ. Sci. Technol.* **2009**, *43*, 718-723.
31) Rodgers, M. A. J.; Snowden, P. T. Lifetime of $^{1}O_2$ in liquid water as determined by time-resolved infrared luminescence measurements. *J. Am. Chem. Soc.* **1982**, *104*, 5541-5543.
32) Canonica, S.; Freiburghaus, M. Electron-rich phenols for probing the photochemical reactivity of freshwaters. *Environ. Sci. Technol.* **2001**, *35*, 690-695.
33) Gerecke, A. C.; Canonica, S.; Müller, S. R.; Scharer, M.; Schwarzenbach, R. P. Quantification of dissolved natural organic matter (DOM) mediated phototransformation of phenylurea herbicides in lakes. *Environ. Sci. Technol.* **2001**, *35*, 3915-3923.
34) Canonica, S.; Hellrung, B.; Müller, P.; Wirz, J. Aqueous oxidation of phenylurea herbicides by triplet aromatic ketones. *Environ. Sci. Technol.* **2006**, *40*, 6636-6641.
35) Maddigapu, P. R.; Bedini, A.; Minero, C.; Maurino, V.; Vione, D.; Brigante, M.; Mailhot, G.; Sarakha, M. The pH-dependent photochemistry of anthraquinone-2-sulfonate. *Photochem. Photobiol. Sci.* **2010**, *9*, 323-330.
36) Vione, D.; Minella, M.; Minero, C.; Maurino, V.; Picco, P.; Marchetto, A.; Tartari, G. Photodegradation of nitrite in lake waters: Role of dissolved organic matter. *Environ. Chem.* **2009**, *6*, 407-415.
37) Vione, D.; Das, R.; Rubertelli, F.; Maurino, V.; Minero, C. Modeling of indirect phototransformation reactions in surface waters. In: *Ideas in Chemistry and Molecular Sciences: Advances in Synthetic Chemistry*, Pignataro, B. (ed.), Wiley-VCH, Weinheim, Germany, 2010, pp. 203-234.
38) Chiron, S.; Comoretto, L.; Rinaldi, E.; Maurino, V.; Minero, C.; Vione, D. *Chemosphere* **2009**, *74*, 599-604.

Captions to the Figures

Figure 1. a) Absorption spectra of DCNP (molar absorption coefficient ε) at different pH values. Emission spectrum (spectral photon flux density) of the adopted UVA lamp (Philips TL K05).

b) Absorption spectra of AQ2S and RB (molar absorption coefficient ε). Emission spectra of the UVA (Philips TL K05) and blue (Philips TL K03) lamps.

Figure 2. Time evolution of 20 µM DCNP upon UVA irradiation, at pH 2.3 (adjusted with $HClO_4$) and 7.8 (adjusted with NaOH). The solid lines represent the pseudo-first order exponential fit functions, the dashed ones are the corresponding 95% confidence limits.

Figure 3. Initial transformation rates of 20 µM DCNP upon UVB irradiation of 10 mM $NaNO_3$, as a function of the concentration of added 2-propanol. The solution pH was 8.5, adjusted with NaOH.

Figure 4. Initial transformation rates of DCNP upon irradiation of 20 µM RB under the blue lamp, as a function of the DCNP concentration. The solution pH was 8, adjusted with NaOH.

Figure 5. Initial transformation rates under UVB irradiation of: ( ) 20 µM DCNP and 10 mM $NaNO_3$, as a function of the concentration of $NaHCO_3$; (▲) 20 µM DCNP and 10 mM $NaNO_3$, as a function of the concentration of added phosphate buffer (same concentration as $NaHCO_3$ and same pH, within 0.1 units); (o) 20 µM DCNP, without nitrate, as a function of $NaHCO_3$ concentration.

Figure 6. Initial transformation rates of 20 µM DCNP upon UVA irradiation of 1 mM AQ2S, as a function of the concentration of DCNP. The solution pH was 8.5, adjusted with NaOH.

Figure 7. a) Modelled pseudo-first order degradation constant of DCNP (SSD^{-1} units) as a function of water column depth *d* and NPOC values. The model results are reported for the direct photolysis and the reactions with $^{\bullet}OH$ and $^{1}O_2$. For the model description see the SI.

b) Time evolution of DCP and DCNP in the Rhône delta lagoons (Southern France), after the DCP peak on 21 June (day 0) (*12*). The DCP data were fitted with a pseudo-first order equation, the DCNP ones with equation 14.

Figure 1

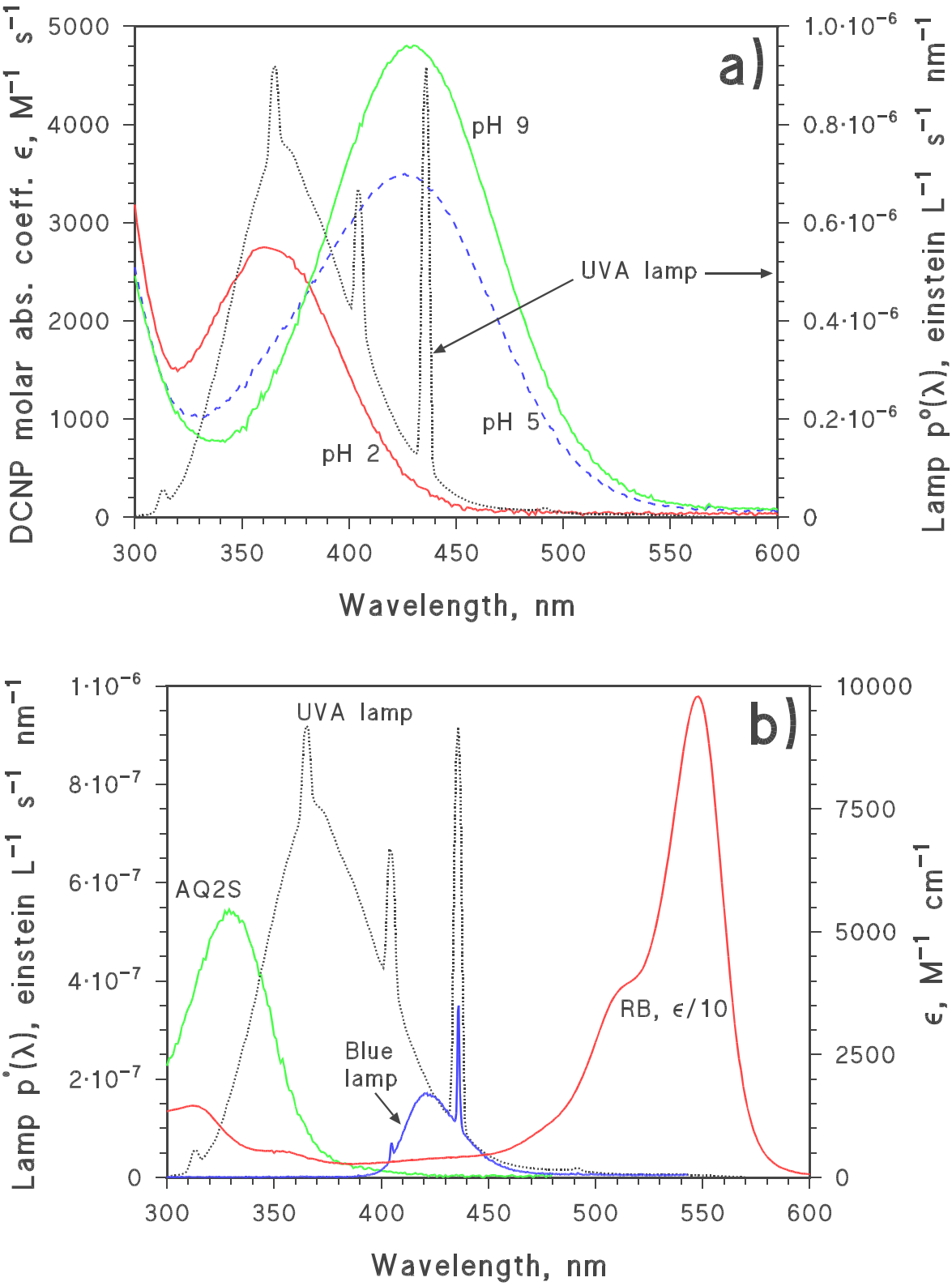
a)
pH 9
pH 5
pH 2
UVA lamp
DCNP molar abs. coeff. ϵ, M⁻¹ s⁻¹
Lamp p°(λ), einstein L⁻¹ s⁻¹ nm⁻¹
Wavelength, nm
b)
UVA lamp
AQ2S
Blue lamp
RB, ϵ/10
Lamp p°(λ), einstein L⁻¹ s⁻¹ nm⁻¹
ϵ, M⁻¹ cm⁻¹
Wavelength, nm

Figure 2

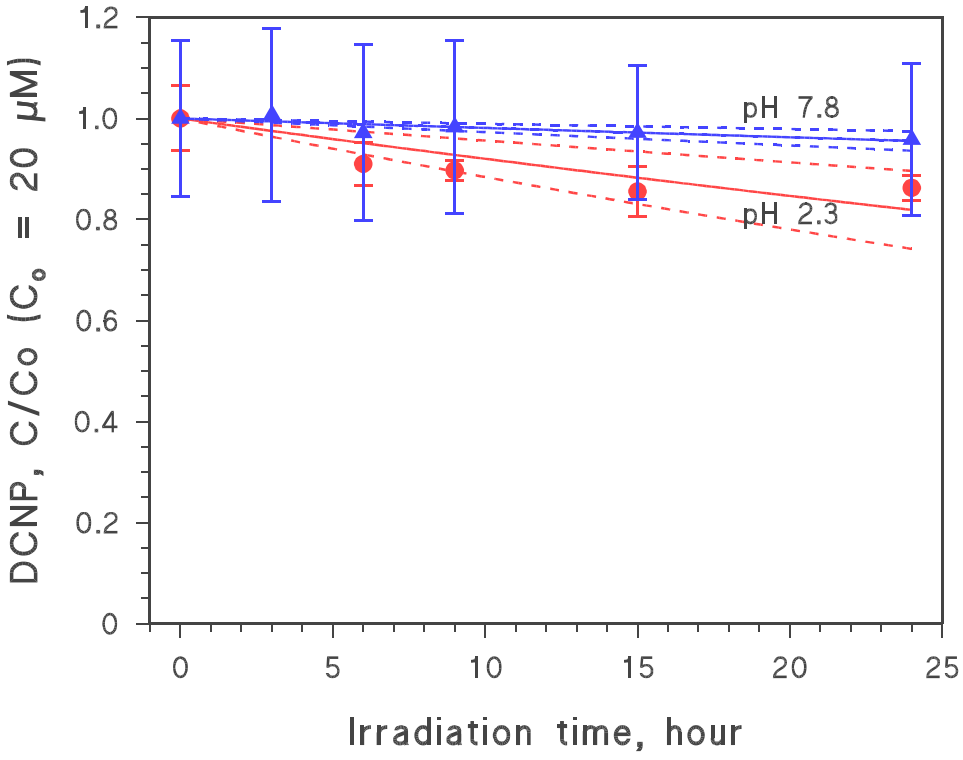
1.2
1.0
0.8
0.6
0.4
0.2
0
DCNP, C/Co (Co = 20 μM)
0
5
10
15
20
25
Irradiation time, hour
pH 7.8
pH 2.3

Figure 3

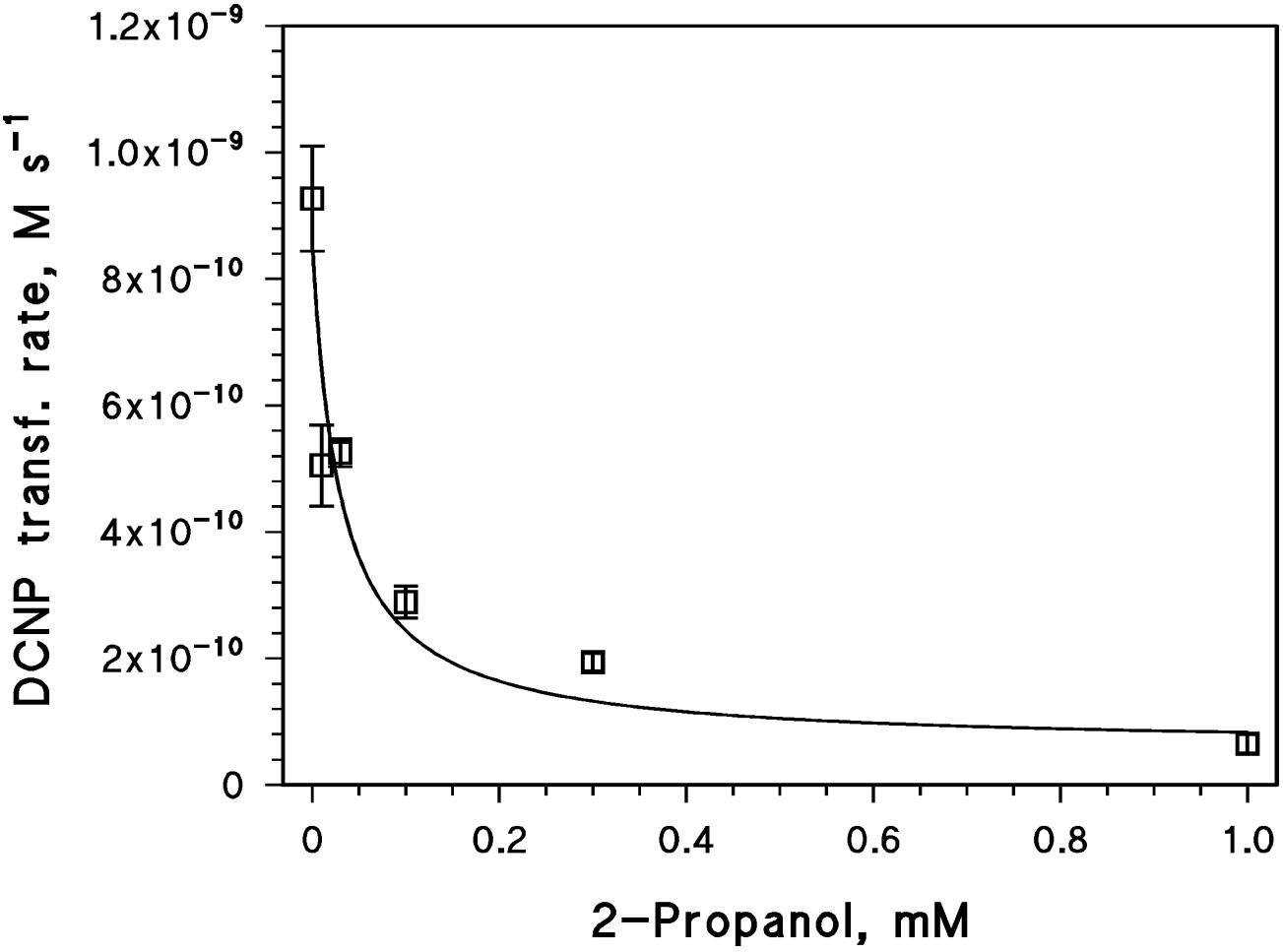
1.2x10⁻⁹
1.0x10⁻⁹
8x10⁻¹⁰
6x10⁻¹⁰
4x10⁻¹⁰
2x10⁻¹⁰
0
DCNP transf. rate, M s⁻¹
0
0.2
0.4
0.6
0.8
1.0
2-Propanol, mM

Figure 4

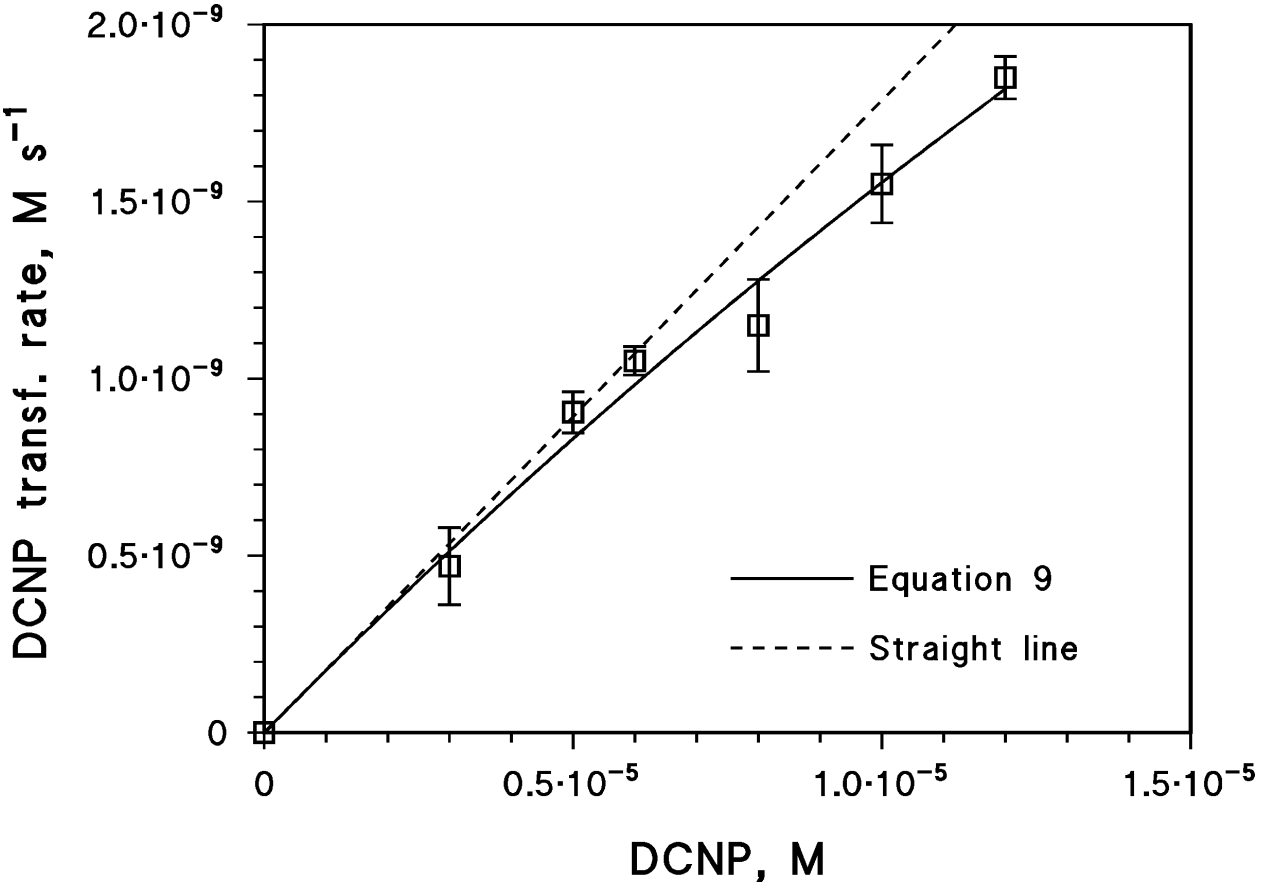
2.0·10⁻⁹
1.5·10⁻⁹
1.0·10⁻⁹
0.5·10⁻⁹
0
DCNP transf. rate, M s⁻¹
0
0.5·10⁻⁵
1.0·10⁻⁵
1.5·10⁻⁵
DCNP, M
Equation 9
Straight line

Figure 5

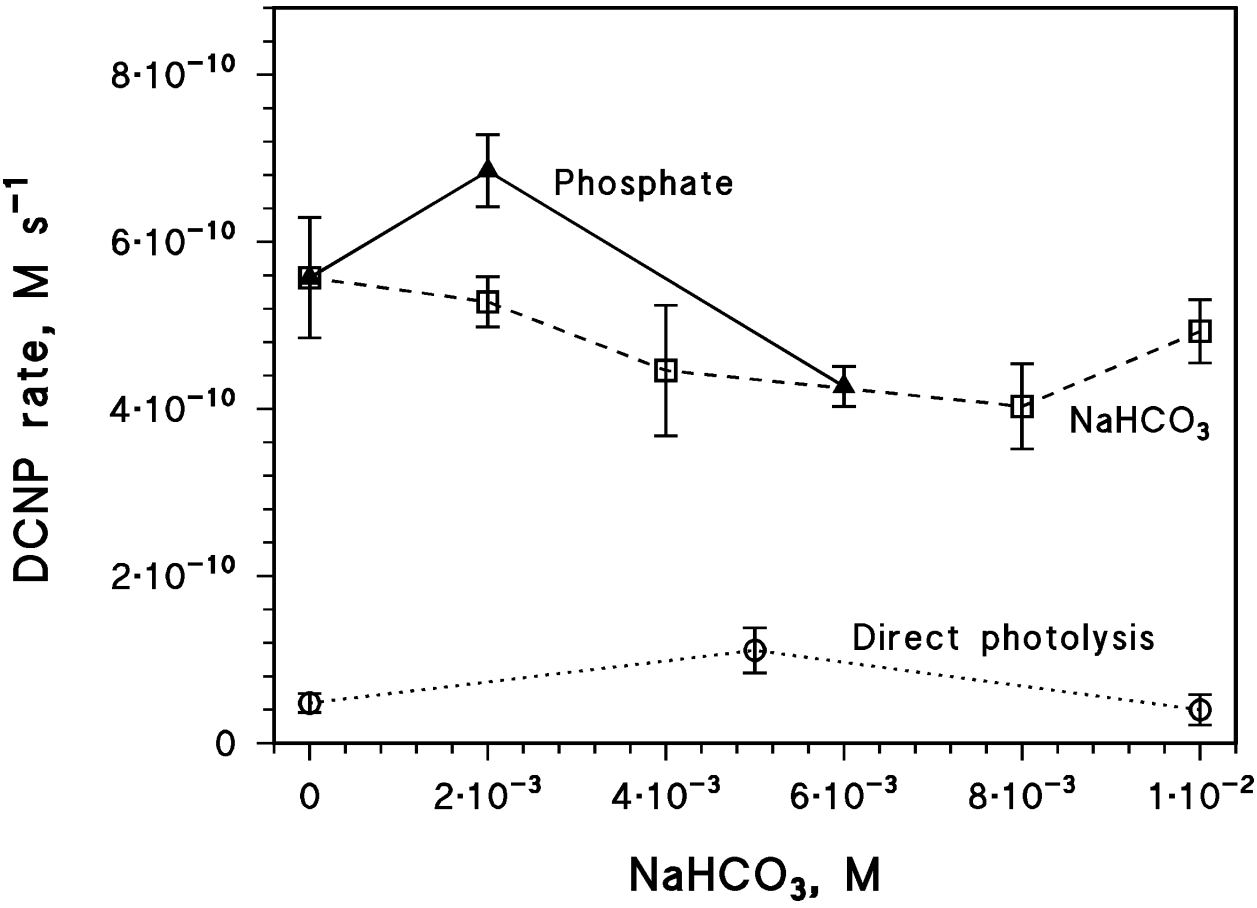
8·10⁻¹⁰
6·10⁻¹⁰
4·10⁻¹⁰
2·10⁻¹⁰
0
DCNP rate, M s⁻¹
Phosphate
NaHCO3
Direct photolysis
0
2·10⁻³
4·10⁻³
6·10⁻³
8·10⁻³
1·10⁻²
NaHCO3, M

Figure 6

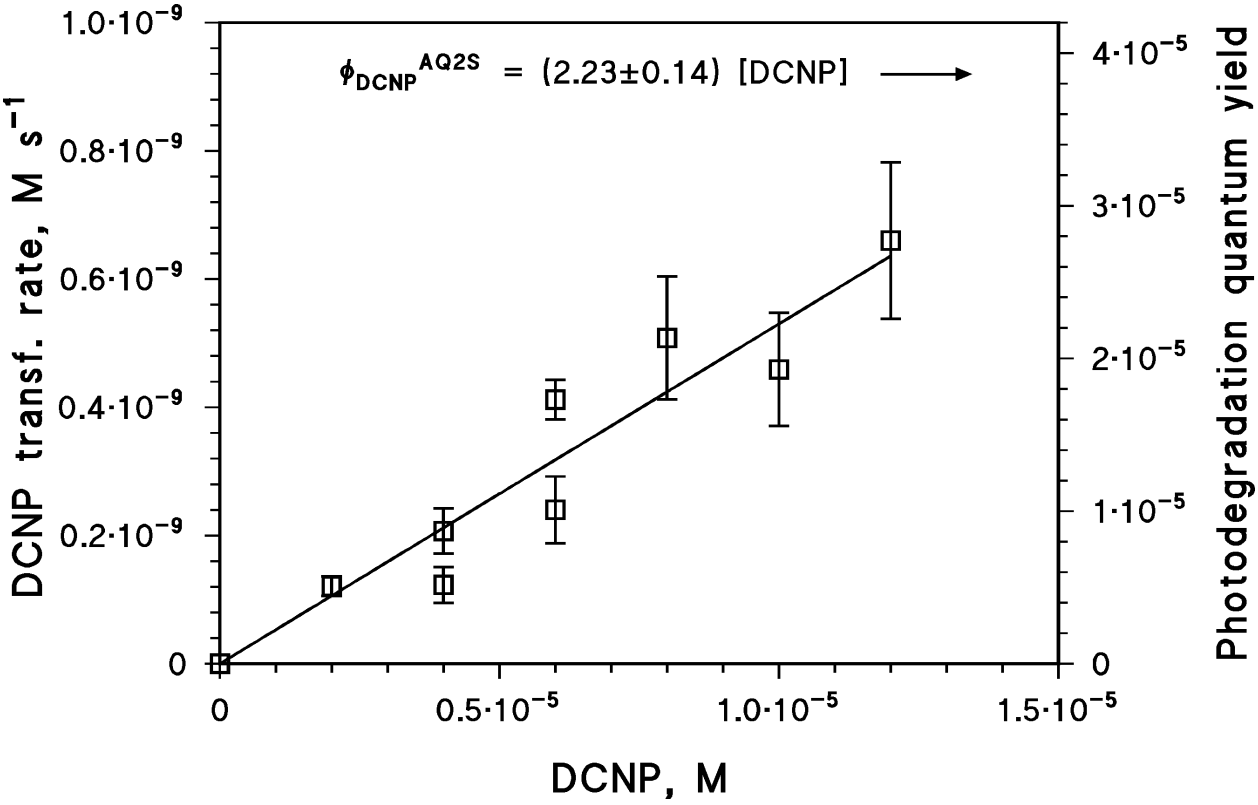
ϕ_{DCNP}^{AQ2S} = (2.23±0.14) [DCNP]
DCNP transf. rate, M s^{-1}
Photodegradation quantum yield
DCNP, M
1.0·10^{-9}
0.8·10^{-9}
0.6·10^{-9}
0.4·10^{-9}
0.2·10^{-9}
0
4·10^{-5}
3·10^{-5}
2·10^{-5}
1·10^{-5}
0
0.5·10^{-5}
1.0·10^{-5}
1.5·10^{-5}

Figure 7

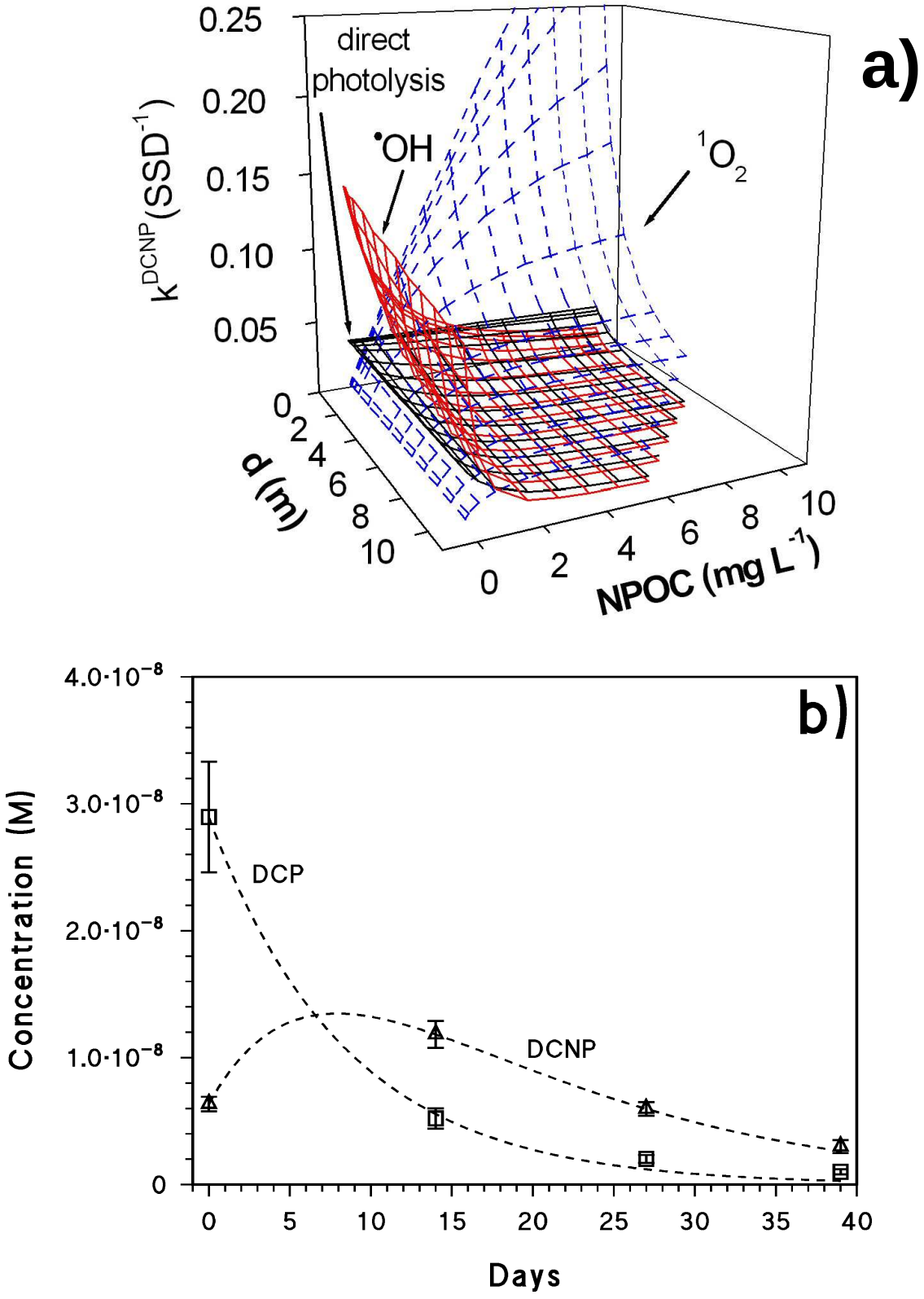
a)
direct
photolysis
•OH
$^1O_2$
$k^{DCNP}(SSD^{-1})$
0.25
0.20
0.15
0.10
0.05
d (m)
0
2
4
6
8
10
NPOC (mg L^{-1})
b)
Concentration (M)
$4.0\cdot10^{-8}$
$3.0\cdot10^{-8}$
$2.0\cdot10^{-8}$
$1.0\cdot10^{-8}$
0
DCP
DCNP
0
5
10
15
20
25
30
35
40
Days